Strong interaction between a fluorescent β-diketone derivative and alkali and alkaline earth cations in solution studied by spectrophotometry

Suzanne Fery–Forgues,*[a] Dominique Lavabre[a] and Alexandre D. Rochal[b]

[a] *Laboratoire des Interactions Moléculaires et Réactivité Chimique et Photochimique, Université Paul Sabatier, 118 route de Narbonne, 31062 Toulouse cedex, France*
[b] *Institute of Chemistry, Kharkov State University, 310077 Kharkov, Ukraine*

The enol form of 3-acetoacetyl-7-methyl-2*H*,5*H*-pyrano(4,3-*b*)pyran-2,5-dione displays interesting spectroscopic characteristics. Therefore, to study its interactions with alkali and alkaline earth perchlorates in acetonitrile, absorption and fluorescence spectroscopies were employed. The presence of salts resulted in strong variations in the absorption spectrum and in a collapse of the fluorescence intensity. The spectrophotometric data, together with NMR and mass spectrometry, allowed an analysis of the interactions involved. Evidence was obtained for the occurrence of complexes of the E^-M type with lithium salts and of the E^-M and $(E^-)_2M$ types with calcium and magnesium salts, E^- denoting the enolate form of the title compound and M the metal cation. In the E^-M complex, the heterocyclic oxygen atom as well as the two oxygen atoms of the side chain can participate in cation binding, as suggested by semi-empirical PM3 calculations. The association constants vary over many orders of magnitude, depending on the nature of the salt. The calcium and magnesium complexes are far more stable than those usually found for crown-ether-based fluoroionophores in the same solvent.

Forte interaction entre une β-dicétone fluorescente et des cations alcalins et alcalino-terreux en solution étudiée par spectrophotométrie. La forme énol de la 3-acetoacetyl-7-methyl-2*H*,5*H*-pyrano(4,3-*b*)pyrane-2,5-dione montre des propriétés spectroscopiques intéressantes. Aussi, les spectroscopies d'absorption et de fluorescence ont été utilisées pour étudier ses interactions avec des perchlorates de cations alcalins et alcalino-terreux dans l'acétonitrile. La présence de sels entraîne de fortes variations du spectre d'absorption et l'effondrement de l'intensité de fluorescence. Les résultats de la spectrophotométrie, joints à ceux de la RMN et de la spectrométrie de masse permettent d'analyser les interactions mises en jeu. On met ainsi en évidence des complexes du type E^-M avec les sels de lithium et du type E^-M et $(E^-)_2M$ avec les sels de calcium et de magnésium, E^- symbolisant la forme énolate du composé et M le cation métallique. Dans le complexe E^-M, l'oxygène hétérocyclique ainsi que les deux atomes d'oxygène de la chaîne latérale pourraient participer à la complexation du cation, comme le suggèrent les calculs PM3. Les constantes d'association varient de plusieurs ordres de grandeur suivant la nature du sel. Les complexes de calcium et de magnésium sont beaucoup plus stables que ceux habituellement trouvés pour les fluoroionophores basés sur des éthers-couronnes dans le même solvant.

β-Diketones are among the most widely used ligands in coordination chemistry.[1] These compounds can exist in solution as keto and enol tautomers. Since the enolic hydrogen is labile, it can be replaced by a metal cation to form a six-membered chelate ring. The β-diketonate complexes thus formed have been the topic of hundreds of papers and reviews,[1–5] the research being stimulated by the versatility of these compounds as NMR shift reagents,[6,7] laser chelates,[8,9] extraction agents,[10–12] heat stabilizers for polymers, drugs,[13,14] chemical and photochemical[15] catalysts, as well as their use in the manufacture of supra-conductors[16,17] and gas chromatography.[18,19] A few papers have also appeared in which β-diketones have been shown to act as neutral ligands by establishing a coordinative interaction with the metal cation.[20–24]

As far as alkali and alkaline earth metals are concerned, many complexes have been synthesized by reacting directly the electropositive element with hydrocarbyl-substituted β-diketones. The corresponding metal chelates were shown to adopt different structures, at least in the solid state, by varying degrees of hydration and by conformational changes of the organic ligand. However, very little is known about the interactions in solution between β-diketone ligands and these cations. Even more, to our knowledge, no attempt has been made to use β-diketone derivatives as optical probes for the recognition of biologically important cations in solution. This lack of interest probably originates from the fact that many β-diketones do not absorb in the visible part of the wavelength range and that very few fluorescent derivatives of them have been reported until now in the literature,[25] the excitation energy being usually dispersed in a very efficient photoisomerization process.

Recently, a new β-diketone heterocyclic derivative, 3-acetoacetyl-7-methyl-2*H*,5*H*-pyrano(4,3-*b*)pyran-2,5-dione (compound **I**, Scheme 1), was synthesized in this laboratory.[26] This compound was designed so that its enol form absorbs in the visible part of the spectrum and fluoresces quite efficiently. This particularity allowed us to use absorption and emission spectroscopy to investigate the behaviour of this compound in the presence of alkali and alkaline earth cations in acetonitrile. The fitting of the spectroscopic data together with additional techniques allowed us to study the nature of the possible interactions.

* Fax +335 61 25 17 33; e-mail: sff@gdp.ups-tlse.fr

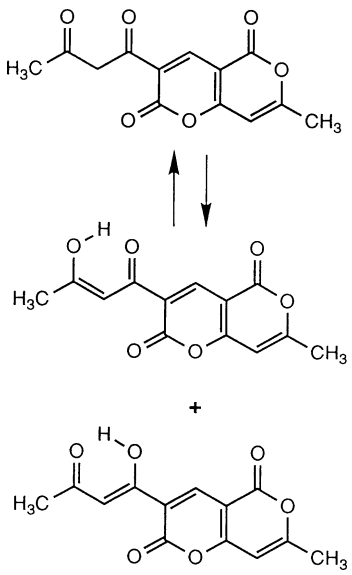

Scheme 1 Compound **I**: equilibrium between the keto (C) and the enol (EH) forms

Results

In an earlier study, it was found that immediately after dissolution in acetonitrile compound **I** exists in a thermal equilibrium between 90% enol and 10% keto forms.[27] Solutions were made and kept in the dark in order to avoid subsequent photoisomerization. Acetonitrile was carefully distilled prior to use, to remove any traces of acid that would otherwise severely interfere with cation binding. Alkali and alkaline earth perchlorate salts were used because they dissolve easily in acetonitrile and do not interfere with the spectrophotometric measurements.

Absorption spectra

The absorption spectrum of free dye **I** has been previously studied.[27] The intense long-wavelength band situated around 390 nm was attributed to the π–π* transition of the enol form, while the band at 280 nm resulted from the absorption of both the enol and the keto forms. In the present work, addition of lithium, magnesium and calcium perchlorates to a solution of **I** (3.2×10^{-6} M) in acetonitrile induced drastic changes in the absorption spectrum. A strong hyperchromic effect on the short-wavelength band (Fig. 1, curves *a* to *c*) was observed. In contrast, the band around 390 nm underwent a hypochromic effect, lost its plateau shape and shifted to the red. The effect was the same for the three cations investigated, although the amount of salt necessary to reach full effect increased in the order Mg < Ca < Li and varied by many orders of magnitude. For comparison, the absorption spectrum of the enolate was recorded by adding sodium hydroxide in an acetonitrile solution of **I** (Fig. 1, curve *d*): only a single band at 440 nm was clearly observed. A similar effect was obtained with different strong bases like triethylamine.

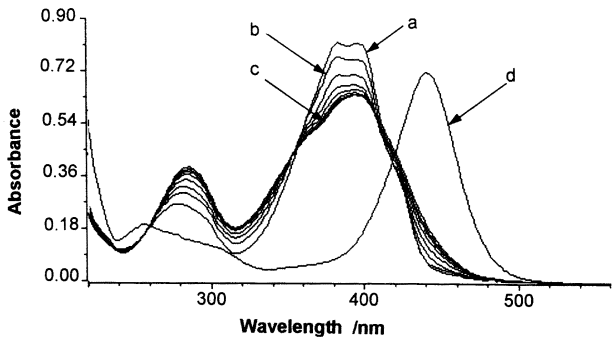

Fig. 1 Absorption spectrum of **I** (3.2×10^{-6} M) in acetonitrile in the absence (curve *a*) and presence of salts. Curves *b* to *c*: effect of calcium perchlorate addition. From top to bottom at 390 nm: $Ca(ClO_4)_2 \cdot 4(H_2O)$: 0.64, 1.3, 1.9, 2.5, 3.2, 3.8, 5.1×10^{-6} M. Curve *d*: effect of sodium hydroxide addition (NaOH at saturation). Cell pathlength: 10 cm

Emission characteristics

It has been previously established[27] that the fluorescence originates from the enol form. Fig. 2 illustrates the evolution of the emission spectrum when increasing the magnesium salt concentration. The strongest effect was observed with this salt and then again, in decreasing order, with calcium and lithium perchlorates. It can be seen that in the presence of perchlorates, the fluorescence intensity of compound **I** strongly decreased without any change in the shape or position of the emission spectrum. Interestingly, in the excitation spectrum the presence of perchlorate salts again had no effect on the shape of the spectrum of compound **I**, which was typically that of the free enol form. However, the excited state lifetime of compound **I** alone in acetonitrile was found to be 0.4 ns and increased to 0.7 ns in the presence of perchlorates.

NMR data

The spectrophotometric variations suggested that definite interactions took place between ligand and metal cation, but whether the complexes involved a neutral (keto or enol) form or an enolate could not be determined. Additional techniques were used to provide more information about the structure of the complexes. The ^1H NMR spectrum of **I** at saturation in CD_3CN was recorded in the presence of 10^{-2} M lithium and magnesium perchlorates and in their absence. In the presence of salts, the most striking effect is that the enol peak, situated at 16 ppm, was strongly reduced with lithium and totally disappeared with magnesium. This suggests that the new species result from the release of the enolic proton, which was replaced by the metal cation. Very weak shifts were observed on the peaks corresponding to the other protons. An identical observation was made when putting **I** in the presence of sodium hydroxide at saturation in the same solvent.

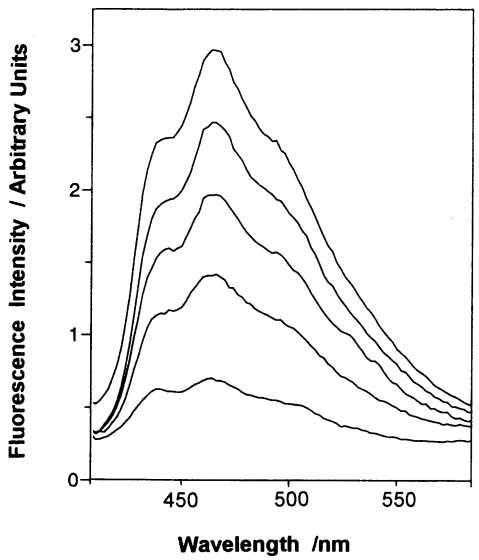

Fig. 2 Effect of the addition of magnesium perchlorate upon the corrected fluorescence spectrum of **I** (3.2×10^{-6} M) in acetonitrile. From top to bottom: $Mg(ClO_4)_2 \cdot 6H_2O$: 0, 0.51, 0.91, 1.4, 2.8×10^{-6} M. Excitation: 358 nm. *T*: 20 °C

Mass spectrometry

The mass spectrum was recorded using the electrospray technique with positive ionization, from a solution of compound **I** and magnesium perchlorate, both at 3×10^{-6} M in acetonitrile. The spectrum is displayed in Fig. 3. No free ligand was detected around $m/z = 262$. The peak at 284.8 can be attributed to the E^-M complex ($C_{13}H_9O_6$, Mg), which may also be solvated by one water molecule (302.9), one acetonitrile molecule (326.3), one molecule of water and one molecule of acetonitrile (344), two molecules of acetonitrile (367), and one molecule of perchloric acid (385–387). Higher mass peaks can be attributed to the $(E^-)_2M$ form [$(C_{13}H_9O_6)_2$, Mg]: the complex with one proton appears at 547, solvation of this protonated complex by one molecule of water or one molecule of acetonitrile gives the peaks at 565 and 588, respectively. The shape of the different signals experimentally found compared favourably with the simulated ones.

Choice of a model and processing of the spectroscopic data

Having spectrophotometric, NMR and mass spectrometry results together induced us to propose the simplest model, which is as follows:

$$EH \underset{k_{-0}}{\overset{k_0}{\rightleftharpoons}} C \quad K_0 = k_0/k_{-0} \qquad (A)$$

$$EH + M \underset{k_{-1}}{\overset{k_1}{\rightleftharpoons}} E^-M + H^+ \quad K_1 = k_1/k_{-1} \qquad (B)$$

$$E^-M + EH \underset{k_{-2}}{\overset{k_2}{\rightleftharpoons}} (E^-)_2M + H^+ \quad K_2 = k_2/k_{-2} \qquad (C)$$

where the free enol, the keto form and the metal cation are represented by EH, C and M, respectively. E^-M and $(E^-)_2M$ are the two complexes of different stoichiometry that can reasonably be considered to be obtained by release of the enolic proton.

At equilibrium, the concentrations of the different species are the solution of the system of equations:

$$K_0[EH] - [C] = 0 \qquad (1)$$

$$K_1[EH][M] - [E^-M][H^+] = 0 \qquad (2)$$

$$K_2[EH][E^-M] - [(E^-)_2M][H^+] = 0 \qquad (3)$$

[C] and [M] are linearly related to the other concentrations by the conservation equations:

$$[C] = [EH]_0 - [EH] - [E^-M] - 2[(E^-)_2M] \qquad (4)$$

$$[M] = [M]_0 - [E^-M] - [(E^-)_2M] \qquad (5)$$

A linear relationship also exists for $[H^+]$ (see *Experimental*):

$$[H^+] = [E^-M] + 2[(E^-)_2M] \qquad (6)$$

Therefore, only the three independent variables [EH], $[E^-M]$ and $[(E^-)_2M]$ remain in eqn. (1), (2) and (3), which can then be solved by an iterative method. The calculations are detailed in the *Experimental*.

The validity of this model was then tested with regard to the spectrophotometric data. The absorption spectra were recorded using cuvettes of 10 cm optical pathlength. This allowed the use of the same concentrations for absorbance measurements as for fluorescence measurements. It was therefore possible to process absorption and fluorescence data simultaneously.

The absorbance and the emission intensity were analysed as a function of cation concentration (Fig. 4). Since the shape of the absorption spectrum varied strongly in the presence of cations, the absorbance was recorded at six different wavelengths chosen in order to obtain maximum information. Meanwhile, since the shape of the emission spectrum remained unchanged, the variation in fluorescence intensity was only measured at 464 nm.

For each salt, the calculation was performed *simultaneously* on the six curves obtained by absorption spectroscopy and on the fluorescence curve (see details in the *Experimental*). The equilibrium constant K_0 was fixed at 0.1 from the NMR data. The values of the equilibrium constants K_1 and K_2 were refined in order to improve the fit between the calculated and the experimental data. Good fits were obtained, as displayed in Fig. 4. The corresponding association constants are reported in Table 1. These values decrease in the order Mg > Ca > Li by several powers of ten. In the case of lithium, only one equilibrium leading to the formation of the complex E^-M was necessary to get an excellent fit. In all cases, convergence was good, whatever the initial values of K_1 and K_2 used. In the case of calcium and magnesium salts, the titration curves are slightly sigmoid and could be fitted only by taking into account the formation of the two complexes E^-M and $(E^-)_2M$. No good fit was obtained by considering only the E^-M-type complex. Convergence was excellent with calcium and only slightly inferior with magnesium. It must be noted that other models were tested, additionally involving complexes like $(E^-M)_2$ or E^-M_2. They did not provide a better fit.

The concentrations of free enol and of the different complexes, for different concentrations of the perchlorate salt, are also shown in Fig. 4. In the case of calcium and magnesium the concentration of complex $(E^-)_2M$ reached a maximum at around 1.8×10^{-6} M of cation and decreased beyond this value, while complex E^-M became preponderant. The calculated spectral characteristics of the complexes are listed in Table 2.

Semi-empirical calculations

Semi-empirical calculations were undertaken in order to better understand the high stability of the possible complexes. The PM3 method was used because it provides for metal atom parameters. In this case, calculations were performed with magnesium as the cation. It was assumed that the interaction involves the electron lone pairs of the oxygen atoms. The stability of the complex therefore increases with the basicity of the oxygen atoms and also depends on the capacity of the ligand molecule to delocalize the charge borne by the metal atom. Heats of formation were calculated for each possible complex, as a measure of the stability of the structure. It must be emphasized that these calculations take into account neither the different hydration and solvation degrees nor the possible interactions with the perchloric acid formed. So, they cannot be taken as more than qualitative.

However, these calculations show that for the E^-M complex the heterocycle oxygen atom may be involved in the complexation. In this case, the heat of formation is slightly

Table 1 Calculated values of the equilibrium constants K_1 and K_2 (dimensionless) and of the ratios $K_i/[H^+]_{av}$ (in M^{-1}), where $[H^+]_{av}$ is arbitrarily taken to be equal to 10^{-6} M

	Li^+	Ca^{2+}	Mg^{2+}
K_1	9.8×10^{-4}	9.3×10^{1}	3.5×10^{3}
K_2	—	1.8×10^{1}	6.3×10^{2}
$K_1/[H^+]_{av}$	9.8×10^{2}	9.3×10^{7}	3.5×10^{9}
$K_2/[H^+]_{av}$		1.8×10^{7}	6.3×10^{8}

Errors were estimated to be around 10%.

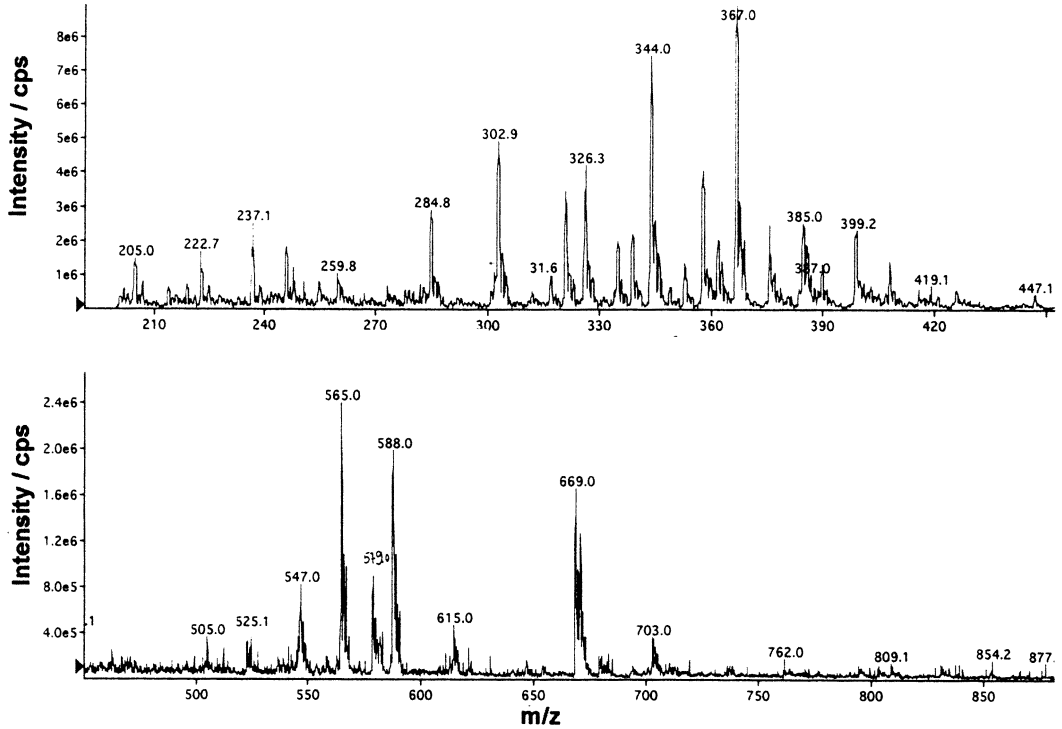

Fig. 3 Mass spectrum of **I** (3×10^{-6} M) in the presence of magnesium perchlorate (3×10^{-6} M) in acetonitrile. Electrospray positive ionization

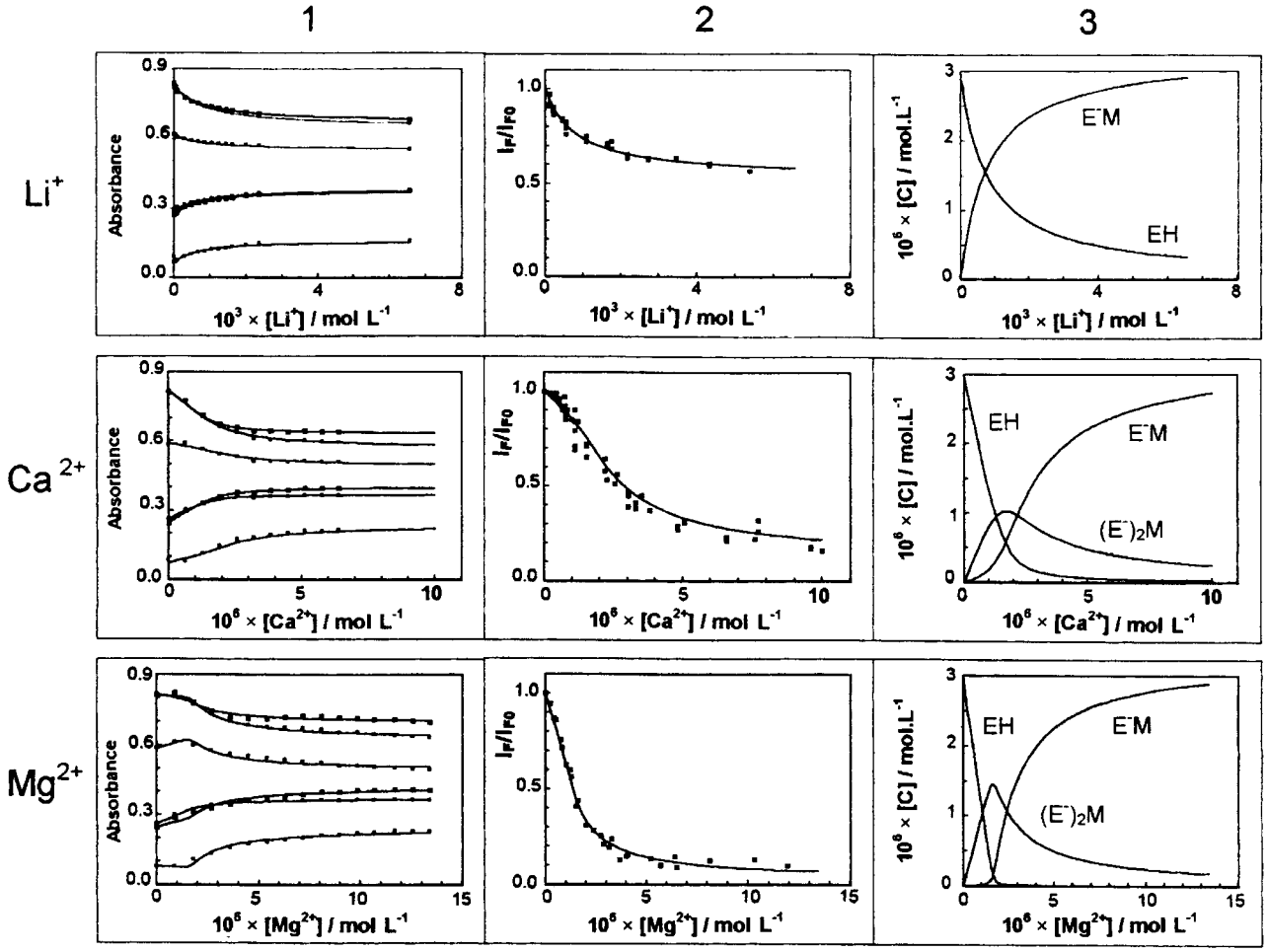

Fig. 4 Fitted spectrophotometric data for compound **I** in acetonitrile *vs.* cation concentration. Column 1: Variation of absorbance. From top to bottom: $\lambda = 396$, 380, 364, 288, 276 and 440 nm. Column 2: Variation of the fluorescence intensity. $\lambda_{ex} = 358$ nm. $\lambda_{em} = 464$ nm. The points are experimental and the curves are calculated by simultaneous fitting of the absorption and fluorescence data for each salt. Column 3: Calculated concentrations of the different species: EH, E^-M and $(E^-)_2M$

Table 2 Molar absorption coefficients ($\varepsilon/M^{-1}\ cm^{-1}$) at different wavelengths and fluorescence quantum yields Φ_F for the free enol (EH) and the pure complexes E^-M and $(E^-)_2M$ obtained with lithium, calcium and magnesium salts

	No salt	Li^+	Ca^{2+}		Mg^{2+}	
	EH	E^-M	E^-M	$(E^-)_2M$	E^-M	$(E^-)_2M$
ε_{276}	8700	12200	11000	20800	11200	19600
ε_{288}	8200	11900	12200	21700	12300	17300
ε_{364}	19300	14900	14400	33100	14800	37600
ε_{380}	26500	16600	16600	39700	18600	47700
ε_{396}	26500	17500	18200	39600	20400	46500
ε_{440}	2300	7000	6800	6500	6200	3800
$\phi/10^{-3}$	3	1	0.26	4.2	0.08	2.2

The values given for the free enol are experimental, those given for the complexes result from calculations.

lower than that found for the structure where only the oxygen atoms of the side chain participate in the bonding (−321 and −319 kJ mol^{-1}, respectively) and the cation bears a much lower charge (+0.80 instead of +0.94). Scheme 2 displays the characteristic geometrical parameters of these complexes. Note that the involvement of the third oxygen atom results in the ligand adopting a rather twisted shape.

In the $(E^-)_2M$ complex, stabilization could be explained by the extensive delocalization of the cation charge ($z_{Mg^{2+}}$ = +0.51). Only the two oxygen atoms of the side chains would participate in the interaction, the coordination centre being symmetrical and every oxygen atom at 1.84 Å from the magnesium atom.

Discussion

Structure of the complexes

Addition of a strong base to compound **I** in acetonitrile readily induced the formation of an enolate. The delocalization of one negative charge over the conjugated system resulted in a strong red-shift of the absorption long-wavelength band together with a hypochromic effect.

In the presence of alkali and alkaline earth cation perchlorates, the absorption spectrum of **I** in acetonitrile solution was neither that of the free enol nor that of the enolate, and did not correspond to the superimposition of the spectra that would be obtained from a mixture of these species. This observation is in line with the formation of a new species involving a cation and compound **I** in its ground state.

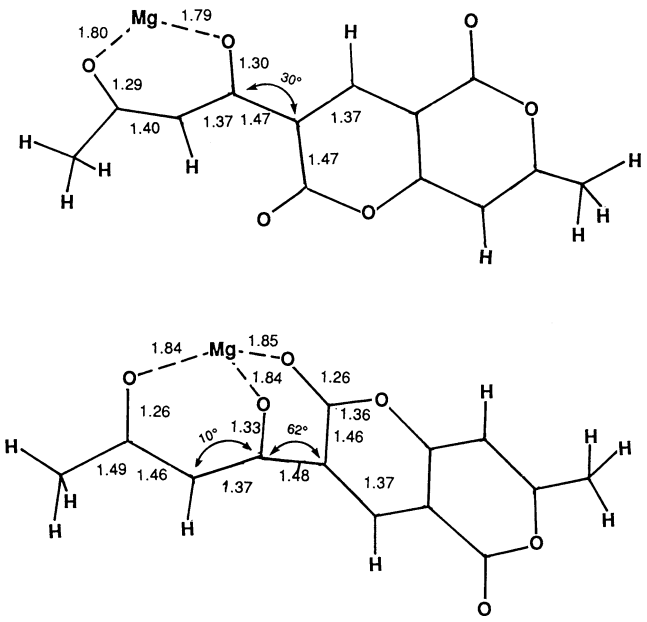

Scheme 2 Calculated bond lengths and angles of interest for complexes E^-M, with two or three oxygen atoms involved in cation binding

From a qualitative viewpoint, this hypothesis was very well-supported by additional techniques: NMR spectroscopy showed that the labile enolic hydrogen disappeared in the presence of salts and mass spectrometry indicated the occurrence of complexes with an E^-M or $(E^-)_2M$ stoichiometry. In such complexes, the charges borne by the atoms would indeed be intermediate between those of the free enol form and those of the free enolate, thus explaining the moderate shift observed in absorption spectroscopy. Semi-empirical calculations suggested that the heterocycle oxygen could participate in cation binding. This could explain that the twisted ligand molecule involved in the E^-M complex thus obtained displays a lower fluorescence quantum yield (Table 2), compared with the almost planar ligand encountered in the $(E^-)_2M$ stoichiometry.

From a more quantitative viewpoint, the model used for the spectrophotometric data analysis is consistent with all the results and also agrees well with the observation that the presence of acidic residues in the solvent inhibits cation binding. The modeling and data analysis used in this work offer the definite advantage that the full set of spectrophotometric data is taken into account. It may be noticed that a simple model, where only the species E^-M and $(E^-)_2M$ were considered, was sufficient to ensure a good fit of the data. However, the presence of higher molecular weight species in low concentrations cannot be ruled out.

The techniques used in this work do not provide any indication concerning the kinetic aspect of complexation.[22,23] In the same way, the exact structure of the complexes formed was not accessible to us. The alkali and alkaline earth metal β-diketonate complexes mentioned in the literature show a propensity for polymorphism.[1,28–30] Their complete characterization relies heavily on X-ray crystallographic data, albeit dissolution in organic solvents may lead to species quite different from the ones obtained in the solid state. The novelty of our work is that these complexes, which appear in solution under very mild conditions, were characterized and studied at concentrations of the diketone derivative and salts as low as 10^{-6} M.

Finally, an interesting point also deserves some attention. For Mg^{2+}, it can be seen in Fig. 4 that the absorbance curve at 364 nm displays a curious shape: the absorbance initially increases and then decreases with rising salt concentration. This behaviour is surprising since the molar extinction coefficient of $(E^-)_2Mg$ at this wavelength (37 600 L $mol^{-1}\ cm^{-1}$) is slightly lower than that corresponding to two molecules of free ligand EH. So the curve should decrease continuously. One explanation is that an important part of the keto form (the proportion of which is 10% in the starting equilibrium)

was enolized and complexed upon addition of metal ions. (Actually, the keto form does not absorb at wavelengths higher than 320 nm, so ε was taken to be equal to zero for the corresponding calculations.)

Stability of the complexes

We now turn our attention towards the association constants. The magnitude of the constants seems to be connected with the charge density of the ion, since it increases in the order Li < Ca < Mg. However, it must be kept in mind that detailed interpretation of this trend may be complicated by the fact that these complexes adopt different coordination spheres. It would have been interesting to compare these constants with those obtained by photometric methods in acetonitrile solutions for a fluoroionophore bearing a monoaza-15-crown-5 ether as the chelating group. Indeed, crown ethers are widely used as building blocks in chromo- and fluoroionophore design since they are considered to be highly efficient for alkali and alkaline earth ion binding. In a previous study, the association constants were found to be 10^4 and 10^2 M^{-1} for calcium and magnesium, respectively.[31] In the present case, the association constant values calculated using our model are dimensionless due to the presence of H^+ in the second member of equilibria (B) and (C). Therefore, they cannot be directly compared to the above estimates.

One can get a good approximation of the sensitivity displayed by compound **I** towards cation binding by observing the fluorescence variation in Fig. 4. Concentrations of magnesium in the range of 10^{-6} M induce a significant effect on a ligand at 3.2×10^{-6} M. In contrast, even in the most favourable cases, concentrations one thousand times higher are necessary to obtain a spectroscopic variation with crown-ether-based chromo- or fluoro-ionophores.

A more quantitative comparison can also be attempted. According to eqn. (6), the average value $[H^+]_{av}$ for the proton concentration can be estimated to be 10^{-6} M, which is the order of magnitude of the concentration range studied. So the ratios: $K_1/[H^+]_{av} = [E^-M]/([EH][M])$ and $K_2/[H^+]_{av} = [(E^-)_2M]/([EH][E^-M])$, expressed in M^{-1}, can now be compared with the binding constants of ref. 31. These values are reported in Table 1. For calcium and magnesium, they are 10^4 and 10^7 times higher than those found for crown-ether-based fluoroionophores.

Actually, the affinity of compound **I** for cations resembles more that of cryptands than that of coronands.[32] Because of their facile synthesis, β-diketone-based molecules could therefore be a very interesting alternative in the design of new cation-sensitive probes. The magnitude of the association constant explains that some β-diketones have been successfully used for alkali and alkaline earth cation extraction,[33] especially when combined with neutral ionophores to obtain a synergistic effect.[34,35]

Photophysical behaviour

As far as the fluorescence properties are considered, the enol form emitted with a fluorescence quantum yield of 3×10^{-3} while the pure enolate form, obtained in the presence of a strong base, was totally non-emissive.[27] In the presence of alkali and alkaline earth perchlorates, emission was observed. As both the emission and excitation spectra are similar to those of the enol form, it is tempting to say that the fluorescence observed in the presence of cations arises from the residual free enol.

However, two observations are not in line with this hypothesis. Firstly, in calculating the amount of free enol remaining in the solution after substantial addition of cations, it becomes evident that this amount is too small to account for the total observed fluorescence. This means that the complexes are fluorescent. Secondly, it is unquestionable that the emission lifetime was significantly longer in the presence of salts. This suggests the involvement of a more complicated mechanism and ultrafast absorption spectroscopy measurements are presently underway in order to get additional information.

Conclusions

In summary, the unusual spectroscopic characteristics of compound **I** allowed us to show that strong interactions take place between **I** and alkali and alkaline earth cations in acetonitrile solutions, at very low concentrations of product and salts. This result was established using complementary techniques: absorption and emission spectrophotometry, NMR and mass spectrometry as well as semi-empirical calculations. In view of the high affinity of the ligand for alkali and alkaline earth cations, this work could lead to the design of new photoactive sensors potentially useful for chemical or biomedical analysis.

Other important consequences of this work can be foreseen at the biological level. Actually, β-diketones are intermediates in the biosynthesis of fatty acids. Given the high association constants found in acetonitrile, it is possible that even in aqueous medium significant interactions take place *in vivo* between β-diketones and cations of biological interest.

Experimental

Materials

3-Acetoacetyl-7-methyl-2*H*,5*H*-pyrano(4,3-*b*)pyran-2,5-dione ($C_{13}H_9O_6$, **I**) was prepared according to a variant of the method described by Boutemeur-Kheddis *et al.*[26] 4-Hydroxy-6-methyl-2-pyrone (2.52 g, 0.02 mole) was dissolved in 30 ml ethanol. After addition of triethyl orthoformate (9 ml, 0.05 mole) and catalytic amounts of potassium cyanide, the reaction mixture was refluxed for 4 h under stirring. After cooling, the precipitate was collected, recrystallized in toluene and sublimed. The yield was 66%. Using this method, 6-methyl-3-(4-hydroxy-6-methyl-2-one-2*H*-pyran-3-yl)methylene-2,4(3*H*)-pyran-2,4-dione, which was identified as a usual byproduct,[36] is not encountered in the final product, which shows high spectroscopic purity.

Spectroscopic grade acetonitrile (Merck) was redistilled over potassium hydroxide prior to use in order to remove traces of acetic acid, discarding the last third of the volume. Only fresh solutions of compound **I** in acetonitrile were used for spectroscopy. It was checked that no enolate form E^- was detected in the UV spectrum (shoulder at 440 nm).

Perchlorate salts $LiClO_4$, $Ca(ClO_4)_2 \cdot 4H_2O$, $Mg(ClO_4)_2 \cdot 6H_2O$) were purchased from Aldrich or Janssen and used as recieved.

Apparatus

Absorbance spectra were recorded on a Hewlett–Packard 8452A diode array spectrophotometer. Steady state fluorescence work was performed on a Photon Technology International (PTI) Quanta Master 1 spectrofluorometer. All fluorescence spectra were obtained by exciting at 358 nm (pseudo-isosbestic point) and were corrected. The fluorescence quantum yields were determined using 4-diethylamino-7-nitrobenzofurazan in dichloromethane ($\Phi_F = 0.038$) as standard.[37] Fluorescence decays were measured with the stroboscopic technique utilizing a Strobe Master fluorescence lifetime spectrometer from PTI. The excitation source was a flash lamp filled with a mixture of nitrogen and helium (30 : 70). Samples were excited at 337 nm and the decay monitored at 464 nm. Data collection was carried over 200 channels with a timebase of 0.1 ns per channel. The measurements were made at 20 °C in a thermostatted cell. Analysis of the fluorescence decay was performed using the monoexponential

method software from PTI. ^{1}H NMR spectra were recorded on a Bruker spectrometer operating at 200 MHz. The mass spectrum was obtained on a simple quadrupole mass spectrometer (Perkin–Elmer Sciex API 100), using electrospray as the ionization mode. The infusion rate was 5 μl min^{-1}.

Data analysis

The spectrophotometric data were processed on a HP 9000 series 710 workstation. The system of eqn. (1), (2) and (3) was numerically solved by an iterative method. Absorbance A was calculated using Beer–Lambert's law at each wavelength considered:

$$A = \Sigma\varepsilon_i c_i l$$

where ε_i and c_i are the molar absorption coefficient and the concentration of species i, respectively, and l is the optical pathway. ε_{EH} and ε_C were measured, ε_{H^+} and ε_M were taken equal to zero. The fluorescence intensity I_F was supposed to be proportional to $\Sigma\phi_i c_i$ where ϕ_i is the fluorescence quantum yield of species i. Note that the excitation wavelength of 358 nm corresponds to a pseudo-isosbestic point where it can reasonably be assumed that the molar absorption coefficients are very similar. Variations of absorbance or fluorescence *vs.* the initial concentration in cation $[M]_0$ can therefore be calculated.

The algorithm used in this method can be summarized as follows. (1) 'Realistic' starting values are chosen for the unknown parameters K_1, K_2, Φ_{E^-M} and $\Phi_{(E^-)_2M}$ as well as for ε_{E^-M} and $\varepsilon_{(E^-)_2M}$ at each wavelength considered. (2) The nonlinear equation system (1), (2) and (3) is solved using an iterative numerical method. Solutions of (2) are used to calculate absorbances and fluorescence intensity. (4) Operations (2) and (3) are repeated for each value of $[M]_0$. Comparison of the numerically calculated absorbances and fluorescence intensities with the experimental values allowed the overall error (sum of the squares of the differences) from the whole set of data to be calculated. (5) The overall error is minimized by a Powell nonlinear minimization algorithm, that is returning to point (1) with better parameters, until the overall error could not be reduced any longer. When optimization is achieved, both a set of adjusted parameters and the concentrations of each species [EH], $[E^-M]$ and $[(E^-)_2M]$ as a function of $[M]_0$ are available.

This widely used method, called 'inverse treatment' presents two distinct advantages: the whole set of experimental data is simultaneously taken into account, and different models can easily be tested by simply changing the starting equations, which makes the method not only able to calculate parameters, but above all to test the validity of various models.

In practice, our software does not use eqn. (1), (2) and (3) but the evolution equations:

$$\begin{aligned} d[EH]/dt = &-k_0[EH] + k_{-0}[C] - k_1[EH][M] \\ &+ k_{-1}[E^-M][H^+] - k_2[EH][E^-M] \\ &+ k_{-2}[(E^-)_2M][H^+] \end{aligned} \quad (7)$$

$$d[E^-M]/dt = k_1[EH][M] - k_{-1}[E^-M][H^+] - k_2[EH][E^-M] + k_{-2}[(E^-)_2M][H^+] \quad (8)$$

$$d[(E^-)_2M]/dt = k_2[EH][E^-M] - k_{-2}[(E^-)_2M][H^+] \quad (9)$$

$$\begin{aligned} d[H^+]/dt = &\, k_1[EH][M] - k_{-1}[E^-M][H^+] \\ &+ k_2[EH][E^-M] - k_{-2}[(E^-)_2M][H^+] \end{aligned} \quad (10)$$

In our case, of course, these equations were not numerically integrated as a function of time but only solved at equilibrium.

Combining eqn. (10) with (8) and (9), one can see that:

$$d[H^+]/dt = d[E^-M]/dt + 2\, d[(E^-)_2M]/dt \quad (11)$$

that is, integrating with the integration constant $[H^+]_0$ assumed to be equal to zero:

$$[H^+] = [E^-M] + 2[(E^-)_2M]$$

which is eqn. (6) used above.

The absorption and emission characteristics of the complexes extracted from the calculation are gathered in Table 2, which reports the molar absorption coefficients calculated for the six wavelengths considered and the fluorescence quantum yields. The values given are averages, resulting from calculations performed using the same model, but starting from different values. Good convergence was obtained for the equilibrium constants K, although variations were observed in the calculated values of ε and Φ. The good convergence obtained for constants K can be explained by the fact that these constants are determined by the shape of the experimental curves (curvature, position of the inflection points, *etc.*) while ε and Φ values only act as scale factors that can compensate each others.

The semi-empirical calculations were performed by using the PM3 method.[38]

Acknowledgements

Dr. M. Hamdi, Dr. V. Spéziale and Ms. K. Vercruysse are thanked for their help in previous preparations of the product. Drs. S. Richelme and M. P. Ferté have acquired the mass spectrum and kindly assisted in its interpretation. We are also indebted to Drs. B. Delavaux-Nicot and F. Alary for fruitful discussions about this work, and to Professor R. Nagarajan for careful rereading of the manuscript.

References

1 A. R. Siedle, in *Comprehensive Coordination Chemistry*, ed. G. Wilkinson, Pergamon Press, Oxford, 1987, vol. 2, ch. 15.4, pp. 365–412.
2 R. C. Mehrotra, R. Bohra and D. P. Gaur, *Metal β-Diketonates and Allied Derivatives*, Academic Press, London, 1978; R. C. Mehrotra, *Pure Appl. Chem.*, 1988, **60**, 1349.
3 J. P. Fackler, *Prog. Inorg. Chem.*, 1966, **7**, 361.
4 S. Kawagushi, *Coord. Chem. Rev.*, 1986, **70**, 51.
5 A. D. Garnovskii, *Koord. Khim.*, 1992, **18**, 675.
6 C. C. Hinckley, *J. Am. Chem. Soc.*, 1969, **91**, 5160.
7 T. J. Wenzel, T. C. Bettes, J. E. Sadlowski and R. E. Sievers, *J. Am. Chem. Soc.*, 1980, **102**, 5903; T. J. Wenzel and J. Zaia, *J. Org. Chem.*, 1985, **50**, 1322.
8 C. Brecher, A. Lempicki and H. Samelson, *J. Chem. Phys.*, 1965, **42**, 1081.
9 L. J. Nugent, M. L. Bhaumik and S. M. Lee, *J. Chem. Phys.*, 1964, **41**, 1305.
10 A. M. Poskanzer and B. M. Foreman., *J. Inorg. Nucl. Chem.*, 1961, **16**, 323.
11 C. Testa, *Anal. Chim. Acta*, 1961, **25**, 525.
12 A. Ikehata and T. Shimizu, *Bull. Chem. Soc. Jpn.*, 1965, **38**, 1385.
13 Y. Anjaneyulu and R. P. Rao, *Synth. React. Inorg. Metal-Org. Chem.*, 1986, **16**, 257.
14 B. K. Keppler, C. Friesen, H. G. Moritz, H. Vongerichten and E. Vogel, *Struct. Bonding* (*Berlin*), 1991, **78**, 97.
15 B. Marciniak and G. E. Buono-Core, *J. Photochem. Photobiol. A: Chem.*, 1990, **52**, 1.
16 L. G. Hubert–Pfalzgraf, *Appl. Organomet. Chem.*, 1992, **6**, 627.
17 R. E. Sievers, S. B. Turnipseed, L. Huang and A. F. Lagalante, *Coord. Chem. Rev.*, 1993, **128**, 285.
18 K. Robards, E. Patsalides and S. Dilli, *J. Chromatogr.*, 1987, **411**, 1.
19 V. A. Komarov, *Zh. Anal. Khim.*, 1976, **31**, 366.
20 P. W. N. M. Van Leeuwen, *Recl. Trav. Chim. Pays-Bas*, 1968, **87**, 396; P. W. N. M. Van Leeuwen and A. P. Praat, *Inorg. Chim. Acta*, 1970, **4**, 101.
21 A. L. Allred and D. W. Thompson, *Inorg. Chem.*, 1968, **7**, 1196.
22 C. A. Blanco and M. J. Hynes, *Can. J. Chem.*, 1992, **70**, 2285.
23 R. G. Pearson and O. P. Anderson, *Inorg. Chem.*, 1970, **9**, 39.
24 D. P. Fay, A. R. Nichols and N. Sutin, *Inorg. Chem.*, 1971, **10**, 2096.

25 K. Gustav and U. Bartsch, *Monatsh. Chem.*, 1991, **122**, 269; *ibid.*, 1991, **122**, 565.
26 B. Boutemeur-Kheddis, A. Bendaas, M. Hamdi, R. Sakellariou and V. Spéziale, *OPPI Briefs*, 1994, **26**, 278.
27 G. Ellingsen, K. Vercruysse, V. Spéziale, M. Hamdi and S. Fery-Forgues, *Acta Chem. Scand.*, 1997, **51**, 521.
28 S. B. Turnipseed, R. M. Barkley and R. E. Sievers., *Inorg. Chem.*, 1991, **30**, 1164.
29 B. A. Uzoukwu., *Inorg. Chim. Acta*, 1990, **176**, 143.
30 A. V. Bogatskii., A. E. Derkach and T. K. Chumachenko, in *Beta-Diketonaty Metallov*, ed. V. I. Spitsyn, Izd. Nauka, Moscow, 1978, pp. 69–72.
31 S. Fery–Forgues, M. T. Le Bris, J. P. Guetté and B. Valeur, *J. Phys. Chem.*, 1988, **92**, 6233.
32 F. Vögtle, *Supramolecular Chemistry*, J. Wiley, Chichester, 1993, p. 43.
33 T. Sekine and N. Thi Kim Dung, *Anal. Sci.*, 1993, **9**, 851.
34 J. H. Kim, E. Kunugita and I. Komasawa, *Kagaku Kogaku Ronbunshu*, 1990, **16**, 1167; *Chem. Abstr.*, 1991, **114**, 10044d.
35 T. Itoh, M. Billah, T. Honjo and K. Terada., *Anal. Sci.*, 1991, **7**, 47.
36 S. Fery–Forgues and K. Vercruysse, unpublished results.
37 S. Fery–Forgues, J. P. Fayet and A. Lopez, *J. Photochem. Photobiol. A: Chem.*, 1993, **70**, 229.
38 J. J. P. Stewart, *J. Comput. Chem.*, 1989, **10**, 209.

Received in Montpellier, France, 7th April, 1998;
Paper 8/02688B